

**GLOBAL MINI-RF S-BAND CPR AND M-CHI DECOMPOSITION OBSERVATIONS OF THE MOON,**  
 Joshua T. S. Cahill<sup>1</sup>, D. Benjamin J. Bussey<sup>1</sup>, G. Wesley Patterson<sup>1</sup>, F. Scott Turner<sup>1</sup>, Norberto R. Lopez<sup>1</sup>, R. Keith Raney<sup>1</sup>, Catherine D. Neish<sup>1</sup>, and the Mini-RF Science Team, <sup>1</sup>JHU-APL, Laurel, MD; (Joshua.Cahill@jhuapl.edu).

**Introduction:** The Lunar Reconnaissance Orbiter (LRO), carries with it NASA’s Miniature Radio Frequency (Mini-RF) instrument which has returned high-quality radar of all regions of the Moon. Mini-RF is a hybrid polarization synthetic aperture radar that showcases the power of radar science in a small package [1]. The observations Mini-RF has collected include nearly complete coverage of the lunar North and South Poles (~99% coverage) and ~67% of the lunar globe. This includes never before observed radar coverage of western Orientale and the farside Feldspathic Highlands and South Pole Aitken basin terranes (FHT and SPA, respectively). These regions are not visible from Earth-based radar observatories such as, Arecibo Radar and Green Bank Telescopes [2]. Here, we present complete spatially uncontrolled Mini-RF global S-band products.

**Instrument:** Mini-RF is a hybrid-polarized, side-looking, synthetic aperture radar (SAR) that transmits both S-band (12.6 cm) and X-band (4.2 cm) wavelengths and operates in two modes: “baseline” at a resolution of 150 m and “zoom” at a resolution of 30 m [1, 3]. Here, we concentrate our analysis on S-band zoom data products which are sensitive to materials 0.1 to 1.26 meters in size and similar vertical depths. The Mini-RF instrument augments previous Earth-based and orbital (i.e., NASA’s Mini-instrument SAR aboard Chandrayaan-1) radar data sets of the Moon collected at 3.8 cm, 12.6 cm and 70 cm [5-9]. Mini-RF’s unique analytical contribution to these data products is its capability to collect data from the entire lunar globe sufficient to determine all four Stokes parameters ( $S_1$ ,  $S_2$ ,  $S_3$ ,  $S_4$ ), or quantitative measurements of polarized radar energy scattered from the lunar surface, at nearly unrestricted viewing geometries [2, 4]. This is a capability Earth-based imaging surveys cannot achieve [4]. Mini-RF data can then be used to compute several analytically valuable child parameters that provide complementary and comparative data to Earth-based products and are familiar to traditional radar astronomers.

**Analysis Method:** Several relevant child parameters are leveraged here for analysis. The most often used is the circular polarization ratio (CPR) which is defined as the ratio of the same sense (SC) relative to the opposite sense (OC) polarized returns. The CPR can also be calculated using the Stokes parameters by,

$$CPR = \frac{(S_1 - S_4)}{(S_1 + S_4)} = \frac{SC}{OC} \quad (1).$$

In this way specular echoes from the lunar surface that are smooth at wavelength scales will return low

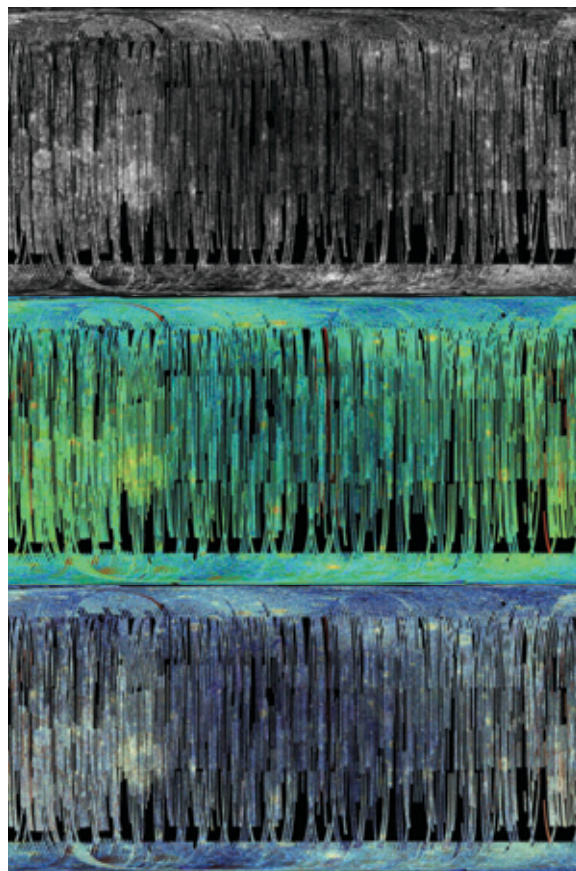


**Figure 1:** Mini-RF  $S_1$  (top), CPR overlaid on  $S_1$  (middle), and  $m$ -chi (bottom) data (10 pixels/degree).

CPR values, while scattering from rough surfaces generate CPR values approaching one or greater. However, this is a simplification and exceptions to this explanation can occur [5]. Therefore, it is important to not rely too heavily on CPR, as its product is informative but can have multiple meanings. Here, other child products are calculated and analyzed to corroborate interpretations. Initial child parameters include the degree of polarization,  $m$ , defined as,

$$m = (S_2^2 + S_3^2 + S_4^2)^{1/2} / S_1 \quad (2)$$

and the degree of circular polarization,  $m_c$ , defined as,

$$m_c = \sin 2\chi = -S_4 / m S_1 \quad (3)$$

where values of  $m$  serve as an indicator of volume versus subsurface scattering.

Another group of parameters that will be used include a combination of child parameters devised by [5]. This is referred to as the  $m$ -chi decomposition where three physical parameters measurements are used. This includes measures of double bounce backscatter (e.g., dihedral, volume ice), randomly

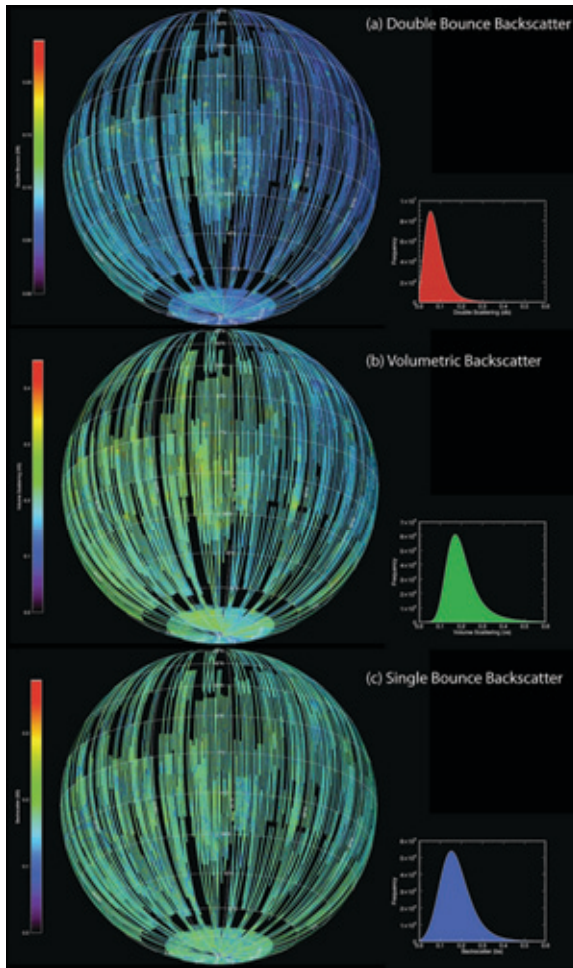


**Figure 2:** Lunar western hemisphere double bounce (a), volume (b), and single bounce (c) backscattering characteristics (64 pixels/degree).

polarized materials (i.e., volume scattering), and finally single bounce backscatter (e.g., Bragg scattering). Double bounce ( $db$ ), volume scattering ( $vs$ ), and single bounce backscatter ( $bs$ ) are described by,

$$\begin{aligned} R &= db = [mS_1(1 + m_c)/2]^{1/2} \\ G &= vs = [S_1(1 - m)]^{1/2} \\ B &= bs = [mS_1(1 - m_c)/2]^{1/2} \end{aligned} \quad (4)$$

within an RGB image, respectively (Fig. 2 and 3).

**Results and Discussion:** Mini-RF mapping of the global Moon suggest a wide range of CPR values (0 – 1.5). Some lunar terranes, such as the Procellarum KREEP Terrane (PKT), are easily differentiated by low backscatter and are spatially consistent with previous terrane designations based upon composition and topography [6, 7] (Fig. 1). For instance, mare basalts of the PKT tend to have a lower backscatter because they are smoother and have higher  $TiO_2$  abundances at depths radar detects. However, other terranes such as the farside SPA and FHT are not as easily differentiated and have relatively similar scattering properties.

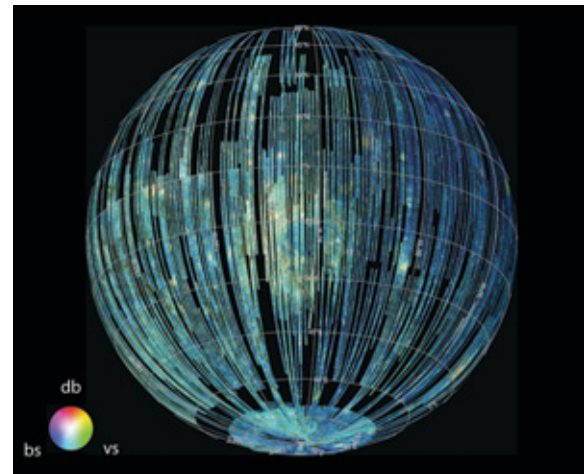


**Figure 3:** Mini-RF  $m$ - $\chi$  decomposition characteristics of the lunar western hemisphere (64 pixels/degree).

This may reflect the age of SPA and its subsection to billions of years of subsequent impact bombardment.

The western hemisphere and Orientale basin is particularly unusual (Fig. 2 and 3). Scattering analyses suggest a relatively uniform Bragg scattering of this hemisphere that, in turn, suggest a regolith consisting of a high density of wavelength scale scatterers blanketing most features. Volumetric scatterers of this hemisphere dominantly reflect regolith depth and maturation and suggest thin, smooth, and Ti-rich mare-like scattering characteristics that reach beyond normal western-PKT boundaries and into eastern and southern Orientale Basin proper and extend to continuous and discontinuous ejecta deposits. Double bounce measurements, a low proportion of the global radar return, refine volumetric scattering interpretations of the western hemisphere suggesting wavelength scale blocks are dominantly confined to the western side of Orientale and Copernican craters of the FHT.

**Summary:** The Mini-RF science team presents uncontrolled global coverage maps of the Moon. Several of these maps are to be delivered to the PDS in the near future and can be used for global analyses of lunar surface/subsurface roughness and inferences regarding surface composition. Semi-controlled global maps comparable in resolution to LROC Wide-Angle Camera (WAC) global maps are now in production.

**References:** [1] Nozette *et al.*, *Space Science Reviews* 150, 285 (2010); [2] Campbell *et al.*, *IEEE Transactions on Geoscience and Remote Sensing* 45, 4032 (2007); [3] Chin, *Space Science Reviews*, (2007); [4] Raney, *Geosci. Rem. Sens. Lett.* 3, 317 (2006); [5] Raney *et al.*, in *Lunar and Planetary Science Conference*. (Lunar and Planetary Institute, Houston, TX, 2012), this volume, ; [6] Jolliff *et al.*, *J. Geophys. Res.-Planets* 105, 4197 (2000); [7] Wieczorek, Phillips, *J. Geophys. Res.-Planets* 105, 20417 (2000);